

Unusual Phosphorus–Phosphorus Double Bond Contraction upon Mono- and Di-auration of a Diphosphene

David V. Partyka,[‡] Marlena P. Washington,[†] Thomas G. Gray,[†] James B. Updegraff III,[†] John F. Turner II,[§] and John D. Protasiewicz^{*†}

Department of Chemistry, Case Western Reserve University, Cleveland, Ohio 44106, Creative Chemistry, LLC, Cleveland, Ohio 44106, and Department of Chemistry, Cleveland State University, Cleveland, Ohio 44115

Received February 3, 2009; E-mail: protasiewicz@case.edu

Abstract: The diphosphene Mes*P=PMes* (Mes* = 2,4,6-tri-*tert*-butylphenyl; **1**) reacted with 1 or 2 equiv of Au(tht)Cl (tht = tetrahydrothiophene) to produce the stable monoaurated adduct Mes*{AuCl}P=PMes* (**2**) or diaurated adduct Mes*{AuCl}P=P{AuCl}Mes* (**3**) respectively. The products were characterized by X-ray crystallography, UV–visible, IR, Raman, and multinuclear NMR spectroscopies, as well as by density functional theory calculations. The crystallographic and Raman spectroscopic data provide physical evidence that the P=P bond grows shorter and increases in strength upon auration; these observations are further examined by DFT calculations for a series of model compounds CH₃{AuCl}_{*n*}P=P{AuCl}_{*n*}CH₃ **1'–3'** (*n*, *n'* = 0 or 1). Compounds **1–3** represent a rare series of crystallographically characterized diphosphenes bearing zero, one, or two AuCl units on each phosphorus atom, allowing for a systematic analysis of the impact of Lewis acids on the phosphorus–phosphorus double bond.

Introduction

Phosphaalkenes (RP=CR'₂)^{1–3} and diphosphenes (RP=PR)^{4,5} represent interesting analogues of olefins (R'₂C=CR'₂) in which one or both of the constituent carbene units (R'₂C) are replaced by phosphinidene units (RP).^{6–8} The parallels between these and other classes of multiply bonded organic compounds have been noted so often that phosphorus has been called a “carbon copy”.⁹ While these similarities are well known, there are some distinct differences that are less well known and understood. One of these that has caught our attention, owing to our interest in preparing extended π -conjugated materials featuring phosphaalkene and diphosphene moieties as participatory π -conjugated elements, is that such materials often display limited or no photoluminescence.^{10,11} For example, while stilbene (Ph(H)C=C(H)Ph) is a well-known fluorescent molecule, analogous molecules having a diphosphene core as a source of fluorescence have not been reported. In fact, Tokitoh and colleagues have shown that the diphosphene Tbt–P=P–(9-Anth) (Tbt = 2, 4, 6-tris[bis(trimethylsilyl)meth-

yl]phenyl) shows only weak fluorescence despite having the anthracene unit.¹² As molecules such as (9-Anth)₃P show little fluorescence, but the related (9-Anth)₃P=O having its lone pair of electrons capped do so,¹³ it has been suggested that the lone pair of electrons on phosphorus in the diphosphene might be quenching fluorescence. Alternatively, changes in the excited state geometry might also cause rapid relaxation.

It is thus of fundamental interest to examine this phenomenon in greater detail. Studies exploiting high-level computational calculations and ultrafast time-resolved spectroscopy indicate that sub-picosecond nonradiative decay involving the phosphorus lone pair electrons is primarily responsible for low fluorescence yield.^{14,15} The role of large-scale conformational changes, including torsional motions about the PP double bond, is also being explored. Some phosphines display a noted positive impact on fluorescence emission for gold binding to phosphorus lone pairs.^{16,17} Here, we investigate the changes that occur when a diphosphene is chemically modified by a Lewis acid (AuCl) in a manner that engages one or both of the lone pairs of electrons on phosphorus.

For this study, the diphosphene Mes*P=PMes* (**1**, Mes* = 2,4,6-tri-*tert*-butyl) was chosen. This landmark molecule, introduced by Yoshifuji in 1981,¹⁸ has also become a benchmark

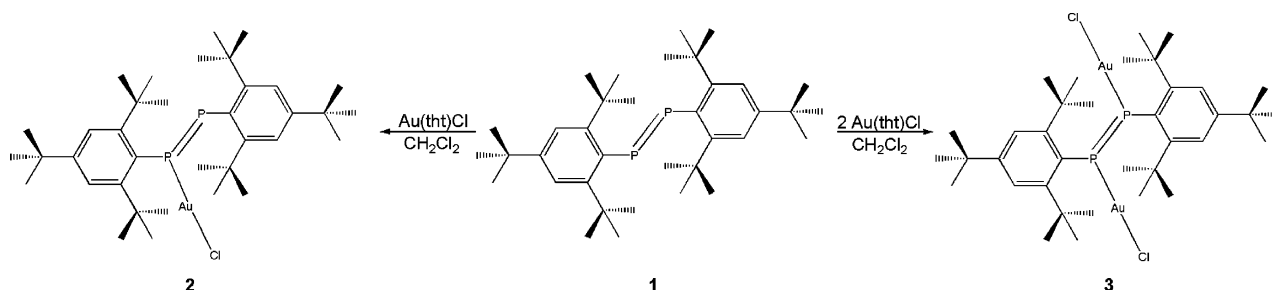
[†] Case Western Reserve University.

[‡] Creative Chemistry, LLC.

[§] Cleveland State University.

- (1) Appel, R.; Knoll, F. *Adv. Inorg. Chem.* **1989**, *33*, 259–361.
- (2) Markovski, L. N.; Romanenko, V. D. *Tetrahedron* **1989**, *45*, 6019–6090.
- (3) Mathey, F. *Acc. Chem. Res.* **1992**, *25*, 90–96.
- (4) Weber, L. *Chem. Rev.* **1992**, *92*, 1839–1906.
- (5) Power, P. P. *Chem. Rev.* **1999**, *99*, 3463–3503.
- (6) Lammertsma, K. *Top. Curr. Chem.* **2003**, *229*, 95–119.
- (7) Mathey, F. *Angew. Chem., Int. Ed.* **2003**, *42*, 1578–1604.
- (8) Power, P. P. *J. Chem. Soc. Dalton. Trans.* **1998**, 2939–2951.
- (9) Dillon, K. B.; Mathey, F.; Nixon, J. F. *Phosphorus: The Carbon Copy*; John Wiley and Sons: New York, 1998.
- (10) Smith, R. C.; Chen, X.; Protasiewicz, J. D. *Inorg. Chem.* **2003**, *42*, 5468–5470.
- (11) Smith, R. C.; Protasiewicz, J. D. *J. Am. Chem. Soc.* **2004**, *126*, 2268–2269.

- (12) Sasamori, T.; Tsurusaki, A.; Nagahora, N.; Matsuda, K.; Kanemitsu, Y.; Watanabe, Y.; Furukawa, Y.; Tokitoh, N. *Chem. Lett.* **2006**, *35*, 1382–1383.
- (13) Yamaguchi, S.; Akiyama, S.; Tamao, K. *J. Organomet. Chem.* **2002**, *646*, 277–281.
- (14) Peng, H.-L.; Payton, J. L.; Protasiewicz, J. D.; Simpson, M. C. *J. Phys. Chem. A* **2009**, *113*, 7054–7063.
- (15) Amatatsu, Y. *J. Phys. Chem. A* **2008**, *112*, 8824–8828.
- (16) Yip, J. H. K.; Prabhavathy, J. *Angew. Chem., Int. Ed.* **2001**, *40*, 2159–2162.
- (17) Lin, R.; Yip, J. H. K.; Zhang, K.; Koh, L. L.; Wong, K.-Y.; Ho, K. P. *J. Am. Chem. Soc.* **2004**, *126*, 15852–15869.

Scheme 1. Syntheses of Aurated Diphosphenes **2** and **3**

diphosphene for an array of studies involving multiply bonded main group compounds.⁴ More recent studies particularly relevant to our work include a combined high-level computational and EDD analysis by Cowley to examine the electronic structure of **1**.¹⁹ In this investigation, a long-standing question on the ordering of the HOMO and HOMO-1 was addressed for **1**. In the UV-vis spectra, two transitions are noted, a $n_+ \rightarrow \pi^*$ and a $\pi \rightarrow \pi^*$, with the latter proposed as the higher energy transition owing to its greater intensity. The EDD/DFT study indicated that the lone pairs on phosphorus make a major contribution to the HOMO, and that the phosphorus-phosphorus π -bond is slightly lower in energy than the n_+ combination of the lone pairs. Another recent computational study indicates that the ordering of these levels is dependent on the extent of conjugation of the aromatic groups with the $P=P$ π system may also be important.¹⁴

As the lone pairs of electrons are clearly positioned to be involved in the photochemistry of diphosphenes, one might suspect that they could play a role in influencing photoluminescence properties. Azobenzenes ($RN=NR$) are also structurally related to diphosphenes, and have been extensively studied for their photochemical properties. A recent report has demonstrated that introduction of an *ortho*- $B(C_6F_5)_2$ group onto azobenzene increases fluorescence intensity by a factor of 30 000.²⁰

While diphosphenes bearing one or more transition metal complexes are known, the impact on fluorescence properties does not appear to have been noted. In addition, owing to the immense size of the Mes* groups in **1**, creating materials having two P-bound transition metal groups is difficult. Diphosphenes having smaller R groups allow coordination of two transition metal centers but often at the expense of being unable to isolate monoadducts. In this article, we report the synthesis and isolation of both monoaurated ($Mes^*\{AuCl\}P=PMe^*$, **2**) and diaurated ($Mes^*\{AuCl\}P=P\{AuCl\}Mes^*$, **3**) adducts of **1**. While no significant increases in fluorescence properties was found, these studies instead reveal unusual phosphorus-phosphorus bond shortening. Possible explanations for the structural impacts of these Lewis acids on a diphosphene are explicated. Such effects do not appear to have been reported for aurated phosphalkenes that are receiving increased attention.^{21–27}

Experimental Section

All solvents and reagents were used as received. Diphosphene **1** was prepared according to the literature procedure.¹⁸ Compounds

2 and **3** were prepared under nitrogen within an MBraun Unilab 2000 inert atmospheres drybox. Microanalyses (C, H, and N) were performed by Quantitative Technologies Inc. All NMR spectra (1H and $^{31}P\{^1H\}$) were recorded in $CDCl_3$ on a Varian AS-400 spectrometer operating at 399.7 and 161.8 MHz, respectively. Raman spectra of **2** and **3** were generated using a 532 nm compact diode laser source at Cleveland State University. UV-vis and fluorescence data were recorded using a Cary 5G UV-vis-NIR spectrometer and a Cary Eclipse spectrometer, respectively.

[Mes*P=P{AuCl}Mes*] (2). An orange solution of **1** (23.3 mg, 0.042 mmol) in 1.5 mL of dichloromethane was added dropwise to a solution of tetrahydrothiophenogold(I) chloride (13.5 mg, 0.042 mmol) in 1.5 mL of dichloromethane. The mixture became yellow and was stirred 1 h. The solvent was then removed by rotary evaporation. The resulting yellow solid **2** was washed with cold (-25 °C) pentane and then collected and dried. Yield: 31 mg (94%). 1H NMR: δ 7.48 (s br, 2H, aromatic), 7.46 (s br, 2H, CH aromatic), 1.60 (s, 18H, *o*- $C(CH_3)_3$), 1.48 (s, 18H, *o*- $C(CH_3)_3$), 1.40 (s, 9H, *p*- $C(CH_3)_3$), 1.35 (s, 9H, *p*- $C(CH_3)_3$). $^{31}P\{^1H\}$ NMR: δ 386.0 (d, 1P, $^1J(P-P) = 538$ Hz), 338.8 (d, 1P, $^1J(P-P) = 539$ Hz). IR (KBr): 648 (m, $\nu_{P=P}$) cm^{-1} . Raman (neat powder, 532 nm excitation): 645 ($\nu_{P=P}$) cm^{-1} . UV-vis (CH_2Cl_2 , 1.88×10^{-5} M): λ (ϵ , $M^{-1} cm^{-1}$) 277 (18 600), 338 (4800), 427 (800) nm. MP: Slow decomposition (turns brown) ~ 80 – 160 °C. A recrystallized sample (chlorobenzene/pentane) gave a satisfactory microanalysis. Anal. Calcd for $C_{36}H_{58}AuClP_2$: C, 55.07; H, 7.45. Found: C, 55.37; H, 7.31.

[Mes*{AuCl}P=P{AuCl}Mes*] (3). An orange solution of **1** (30 mg, 0.054 mmol) in 1.5 mL of dichloromethane was added dropwise to a solution of tetrahydrothiophenogold(I) chloride (34.7 mg, 0.11 mmol) in 1.5 mL of dichloromethane. The solution became yellow and was stirred 1 h. The solvent was removed by rotary evaporation. Analytically pure yellow solid **3** was obtained after trituration with pentane and drying. Yield: 48 mg (87%). 1H NMR: δ 7.55 (s, 4H, aromatic CH), 1.60 (s, 36H, *o*- $C(CH_3)_3$), 1.40 (s, 18H, *o*- $C(CH_3)_3$). $^{31}P\{^1H\}$ NMR: δ 291.3 (s, 2P). Raman (neat powder, 532 nm excitation): 683 ($\nu_{P=P}$) cm^{-1} . UV-vis (CH_2Cl_2 , 2.9×10^{-5} M): λ (ϵ , $M^{-1} cm^{-1}$) 266 (21 000), 350 (8010), 410 (sh, 3530) nm. MP: Slow decomposition (turns brown) 110–161 °C. Anal. Calcd for $C_{36}H_{58}Au_2Cl_2P_2$: C, 42.49; H, 5.74. Found: C, 42.18; H, 5.52.

Computational Analyses. Spin-restricted density-functional theory (DFT) computations were performed within the Gaussian03

- (18) Yoshifuji, M.; Shima, I.; Inamoto, N.; Hirotsu, K.; Higuchi, T. *J. Am. Chem. Soc.* **1981**, *103*, 4587–4589.
 (19) Cowley, A. H.; Decken, A.; Norman, N. C.; Krüger, C.; Lutz, F.; Jacobsen, H.; Ziegler, T. *J. Am. Chem. Soc.* **1997**, *119*, 3389–3390.
 (20) Yoshino, J.; Kano, N.; Kawashima, T. *J. Chem. Soc., Chem. Commun.* **2007**, 559–561.

- (21) Bedford, R. B.; Hill, A. F.; Jones, C.; White, A. J. P.; Williams, D. J.; Wilton-Ely, J. D. E. *T. J. Chem. Soc., Chem. Commun.* **1997**, 179–180.
 (22) Weber, L.; Dembeck, G.; Loenneke, P.; Stammer, H.-G.; Neumann, B. *Organometallics* **2001**, *20*, 2288–2293.
 (23) Weber, L.; Lassahn, U.; Stammer, H.-G.; Neumann, B.; Karaghiosoff, K. *Eur. J. Inorg. Chem.* **2002**, 327, 2–3277.
 (24) Deschamps, E.; Deschamps, B.; Dormieux, J. L.; Ricard, L.; Mezailles, N.; Le Floch, P. *Dalton Trans.* **2006**, 594–602.
 (25) Freytag, M.; Ito, S.; Yoshifuji, M. *Chem. Asian J.* **2006**, *1*, 693–700.
 (26) Ito, S.; Freytag, M.; Yoshifuji, M. *Dalton Trans.* **2006**, 710–713.
 (27) Ito, S.; Freytag, M.; Liang, H.; Nishide, K.; Yoshifuji, M. *Phosphorus, Sulfur Silicon Relat. Elem.* **2008**, *183*, 555–557.

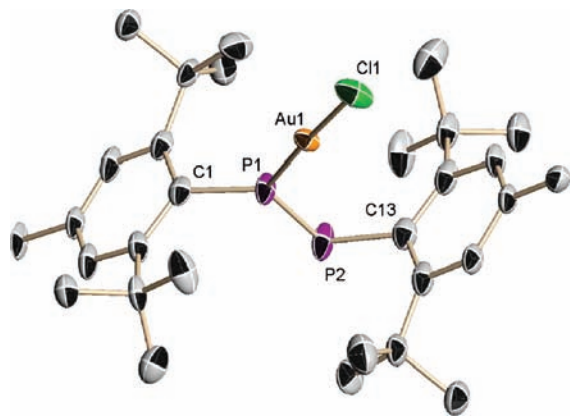


Figure 1. ORTEP representation of **2**, showing 50% probability ellipsoids and selected atom-labeling scheme. Hydrogen atoms, an incompletely resolved *p*-xylene of co-crystallization, and disordered methyl groups of the *p*-*tert*-butyl substituent have been omitted for clarity. Selected bond distances (Å) and bond angles (deg): P1–P2, 1.975(5); Au1–P1, 2.180(4); Au1–C1, 2.222(4); P1–Au1–C1, 177.01(16); Au1–P1–P2, 122.3(2); C1–P1–P2, 106.2(5); C1–P1–Au1, 131.5(5); P1–P2–C13, 99.8(5).

program suite.²⁸ Calculations employed the modified Perdew–Wang exchange functional of Adamo and Barone²⁹ and the original Perdew–Wang correlation functional.³⁰ Gas-phase geometry optimization proceeded using the TZVP basis set of Godbelt, Andzelm, and co-workers.³¹ Gold orbitals were described with the Stuttgart effective core potential and the associated basis set,³² which was contracted as follows, Au, (8s,7p,6d)→[6s,5p,3d]. Harmonic frequency calculations confirmed all converged structures to be potential-energy minima. Relativistic effects with the Stuttgart ECP and its associated basis set are introduced with a potential term (i.e., a one-electron operator) that replaces the two-electron exchange and Coulomb operators resulting from interaction between core electrons and between core and valence electrons. In this way relativistic effects, especially scalar effects, are included implicitly rather than as four-component, one-electron functions in the Dirac equation. Percentage compositions of molecular orbitals, overlap populations, and bond orders between fragments were calculated using the AOMix program.^{33,34} Orbital imaging was performed with the program GaussView 3.0. Orbital contour values are 0.03 au.

X-ray Crystallographic Analyses. Crystals of **2** were grown by vapor diffusion of pentane into a saturated xylenes solution, whereas crystals of **3** were grown by vapor diffusion of pentane into a saturated 1,2-dichloroethane solution. Single-crystal X-ray data were collected on a Bruker AXS SMART APEXII CCD diffractometer using monochromatic Mo K α radiation with ω scan technique. The unit cell was determined using the APEX2 Crystallographic Suite. All structures were solved by direct methods and refined by full matrix least-squares against F^2 with all reflections using SHELXTL. Refinement of extinction coefficients was found to be insignificant. All non-hydrogen atoms were refined anisotropically. All hydrogen atoms were placed in standard calculated positions and were refined with an isotropic displacement parameter 1.5 (CH₃) or 1.2 (all others) times that of the adjacent carbon or nitrogen atom. For **3**, the crystal was found to be merohedrally

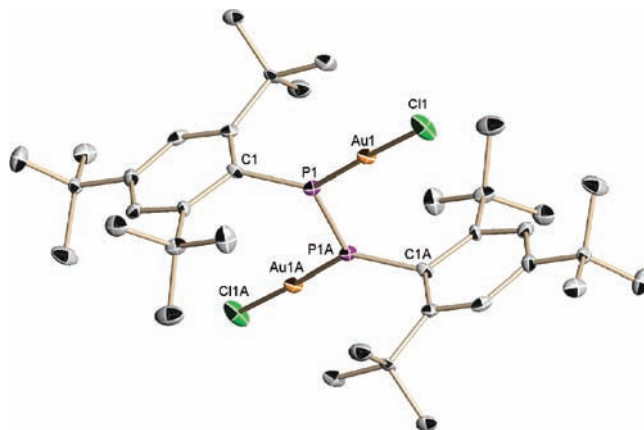


Figure 2. ORTEP representation of **3**, showing 50% probability ellipsoids and selected atom-labeling scheme. Hydrogen atoms have been omitted for clarity. Selected bond distances (Å) and bond angles (deg): P1–P1A, 2.003(4); Au1–P1, 2.201(2); Au1–C1, 2.250(2); P1–Au1–C1, 177.62(9); Au1–P1–P1A, 119.52(16); C1–P1–P1A, 106.0(3); C1–P1–Au1, 134.4(3).

twinning. Cell_Now was used to determine the two individual twin domains. TWINABS was then employed to apply absorption correction and to generate both HCLKF4 and HCLKF5 files. Full refinement was performed using the HCLKF4 file.

Results and Discussion

Cowley and co-workers first reported on the formation of cationic silver and gold adducts of diphosphene **1** by addition of either AgOTf or [Et₃PAu]BF₄.³⁵ While such species were not isolated, the low-temperature (−90 °C) ³¹P NMR data supported the formation of [Mes*{Ag}P=P{Ag}Mes*]OTf₂ (**4a**, δ 355, $^1J_{PP}$ = 480 Hz, $^1J_{PAg}$ = −760 Hz, $^2J_{PAg}$ = 13 Hz) and [Mes*{Ag}P=PMe*]OTf (**4b**, δ 435, 378, $^1J_{PP}$ = 549 Hz, $^1J_{PAg}$ = −751, −750 Hz, $^2J_{PAg}$ = 12, 11.5 Hz) depending on the ratio of AgOTf added to **1**. Addition of [Et₃PAu]BF₄ to **1** led to the identification of [Mes*{Et₃PAu}P=PMe*]OTf (**5**, δ 41.5, 403, 358, $^1J_{PP}$ = 555, −320, 8 Hz). No evidence for a digold dication was found, even upon addition of excess [Et₃PAu]BF₄.

Unlike the cationic silver and gold adducts, neutral gold chloride adducts of **1** can be isolated as stable and crystalline materials. Thus, treating orange solutions of **1** with 1 or 2 equiv of Au(tht)Cl led to an immediate color change from orange to yellow. From these reactions the monoaurated **2** and diaurated **3** could be isolated in high yields as stable solids (Scheme 1). It is noteworthy that **3** is stable for several hours in CDCl₃ solution in air.

In the ³¹P{¹H} NMR (CDCl₃) spectrum of **2**, a pair of doublets centered at δ 339 and 386 ($^1J_{PP}$ = 538 Hz) are located significantly upfield compared to **1** (δ 492), similar to the chemical shifts and PP coupling constant reported for **5**. The ¹H and ³¹P NMR spectra of **3** were much simpler than **2** indicating higher symmetry. A single resonance at δ 291 in the ³¹P NMR spectrum is shifted much further than for either **2** or the disilver dication adduct **4b**.

Single crystal X-ray crystallography rigorously confirmed the identities of **2** and **3**. The results of diffraction studies on **2** are presented in Figure 1. Compound **2** co-crystallizes with one molecule of *p*-xylene per asymmetric unit (not shown). A crystallographically required plane of symmetry containing C1,

(28) Frisch, M. J.; et al. *Gaussian 03, Revision D.01*; Gaussian, Inc.: Wallingford CT, 2004.

(29) Adamo, C.; Barone, V. *J. Chem. Phys.* **1998**, *108*, 664–675.

(30) Perdew, J. P.; Wang, Y. *Phys. Rev. B* **1992**, *45*, 13244–13249.

(31) Godbout, N.; Salahub, D. R.; Andzelm, J.; Wimmer, E. *Can. J. Chem.* **1992**, *70*, 560–71.

(32) Dolg, M.; Wedig, U.; Stoll, H.; Preuss, H. *J. Chem. Phys.* **1987**, *86*, 866–72.

(33) Gorelsky, S. I. *AOMix: Program for Molecular Orbital Analysis*; York University: Toronto, 1997; <http://www.sg-chem.net>.

(34) Gorelsky, S. I.; Lever, A. B. P. *J. Organomet. Chem.* **2001**, *635*, 187–196.

(35) Cowley, A. H.; Norman, N. C.; Pakulski, M. *J. Chem. Soc., Chem. Commun.* **1984**, 1054–5.

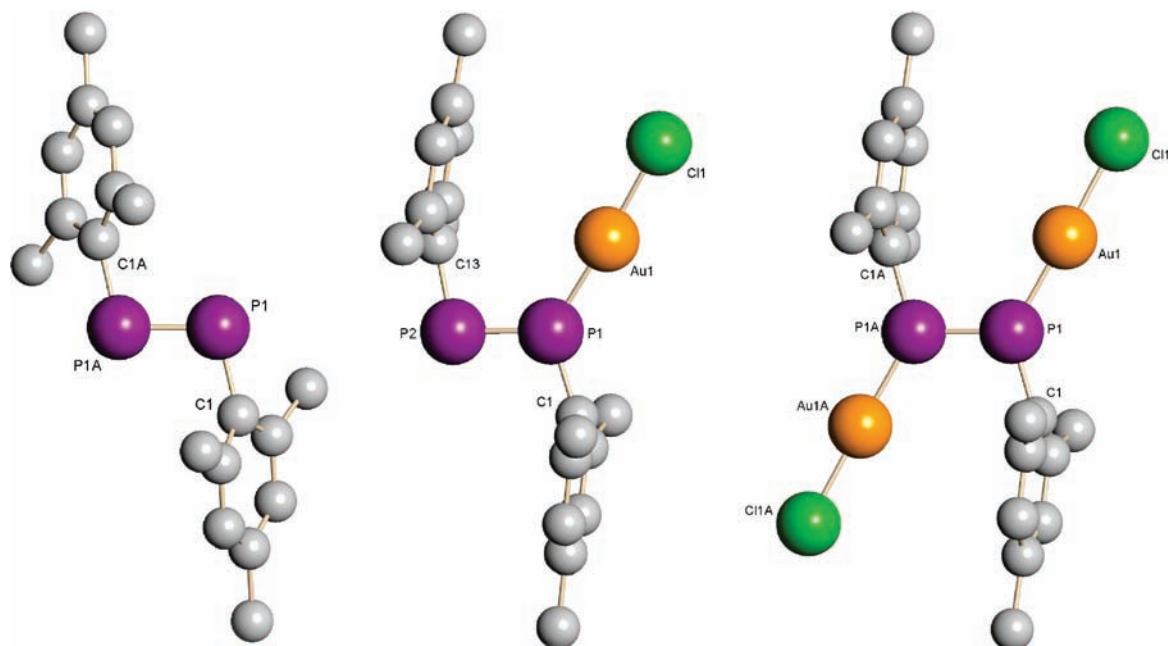


Figure 3. Ball-and-stick comparison of (from left to right) **1–3**. Hydrogen atoms and methyl groups of all *tert*-butyl substituents have been omitted for clarity.

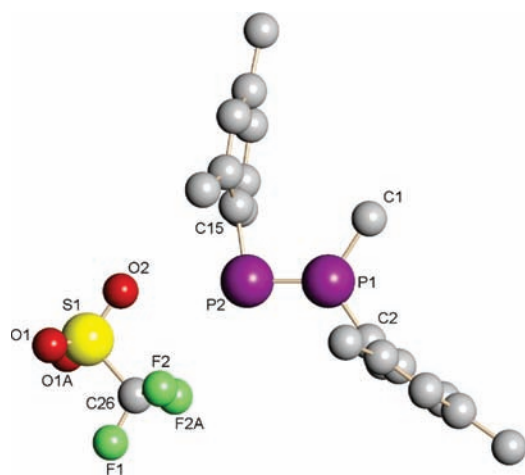


Figure 4. Ball-and-stick comparison of **6** (hydrogen atoms and methyl groups of *tert*-butyl groups removed for clarity).

P1, P2, C13, Au1, and Cl1 relates the two halves of compound **2**, and also dictates planar geometries for both phosphorus atoms. At 1.975(5) Å, the P1–P2 bond length has contracted relative to that for free diphosphene **1**, as determined by either Yoshifuji (2.034(2) Å)¹⁸ or by Cowley (2.047(1) Å).¹⁹

This bond contraction is greater than that found in a methylated version of **1**, [Mes*(Me)P=PMe*s*]OTf (**6**) reported by Grützmacher, which retains a PP double bond and displays a PP bond distance of 2.024(2) Å.³⁶ The ³¹P NMR data for **6** (δ 237, 332.2, $^1J_{PP}$ = 633 Hz) reveal a much greater J_{PP} value (about 100 Hz) than that observed for **2**. Another notable change from the parent diphosphene **1** is that the aromatic rings in **2** are nearly orthogonal to the CPPC plane, while in **1** they are canted by 62°. A distance of 3.45 Å marks a nominally close Au1⋯C1 contact and offers limited evidence for significant gold–aryl interaction.

Crystals of diaurated adduct **3** were also examined by X-ray diffraction, and an ORTEP representation of **3** is shown as Figure 2. A crystallographic center of inversion relates the two halves of **3**, and planar geometries for each phosphorus atom are again realized. Interestingly, **3** also features a shortened PP bond length (2.003(4) Å), albeit not as contracted as found in **2**. The dihedral angle formed by the mean plane of both aryl rings with the C1–P1–P1A–C1A plane is 87°, which again minimizes steric interactions. Similar to **2**, the shortest gold–aryl distance is 3.60 Å, a bit too far to consider as a significant interaction.

Comparative ball-and-stick representations of **1–3** are presented in Figure 3. The most obvious difference between **1** and the aurated diphosphenes is the change in the dihedral angle formed by the aryl planes with the CPPC plane. The CPP bond angles change slightly from 102.4° in **1** to 99.8° and 106.2° in **2** to 106.0° found in **3**. While auration minimally perturbs the C–P=P–C array, methylation and formation of **6** produces greater angular changes, as highlighted in Figure 4. The structure of **6** also features a close O2⋯P2 contact colinear with PP bond. The large P2–P1–C2 bond angle of 123.1(2)°, however, is strikingly greater than that observed for **1–3**. All of these structural details of **2** and **3** (Table 1) are consistent with the retention of a phosphorus–phosphorus double bond. As these materials also have shortened PP bonds, evidence for stronger PP double bonds might be expected by either UV–vis or Raman spectroscopy.

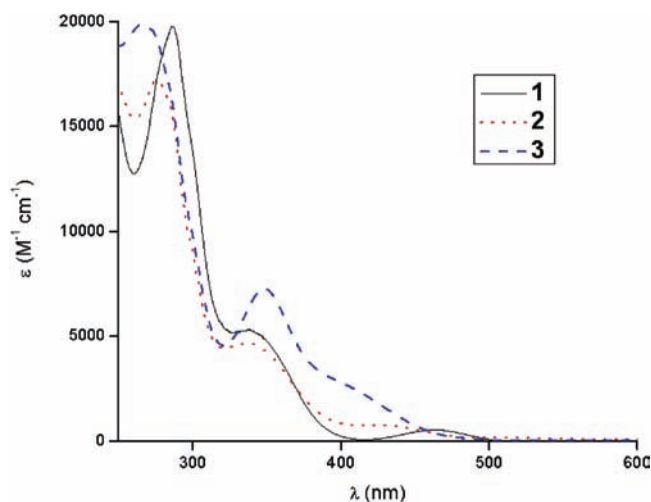
UV–visible spectra of diphosphenes are normally characterized by two transitions close in energy, attributable to $n \rightarrow \pi^*$ and $\pi \rightarrow \pi^*$ transitions. For compound **1** the lower energy (and lower intensity) bands have been assigned as the $n \rightarrow \pi^*$ transition. Absorption spectra of **1–3** were thus recorded in dichloromethane to compare the effects of mono- and diauration of **1**. Figure 5 displays an overlay plot of the spectra. At first glance it appears that monoauration of **1** shifts the $n \rightarrow \pi^*$ transition hypsochromically by 35 to 427 nm, while the $\pi \rightarrow \pi^*$ transition is nearly unchanged at 338 nm. Addition of the second AuCl produces more dramatic changes in the electronic spectra.

(36) Loss, S.; Widauer, C.; Grützmacher, H. *Angew. Chem., Int. Ed. Engl.* **1999**, *38*, 3329–3331.

Table 1. Crystallographic Data for **2** and **3**

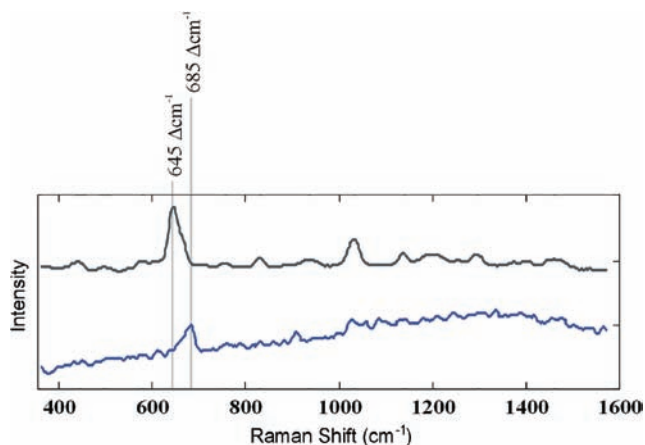
	2	3
formula	C ₃₆ H ₅₈ AuClP ₂ ·C ₈ H ₁₀	C ₃₆ H ₅₈ Au ₂ Cl ₂ P ₂
fw	854.22	1017.60
cryst syst	monoclinic	triclinic
space group	C2/m	P1
a, Å	23.061(10)	8.8414(13)
b, Å	13.414(10)	9.2149(14)
c, Å	14.877(10)	12.2231(14)
α, deg	–	99.969(2)
β, deg	127.395(10)	99.410(2)
γ, deg	–	99.408(3)
cell volume, Å ³	3656(4)	949.6(2)
Z	4	1
D _{calcd} , Mg, m ³	1.552	1.779
T, K	100(2)	100(2)
μ, mm ⁻¹	4.214	7.964
F(000)	1732	496
cryst size, mm ³	0.29 × 0.14 × 0.10	0.16 × 0.14 × 0.09
θ _{min} , θ _{max} , deg	1.72, 26.45	2.29, 27.25
no. of reflns collected	18 393	4164
no. of indep reflns	3296	3831
no. of refined params	232	199
GOF on F ^{2a}	1.281	1.121
R1 [I > 2σ(I)] ^b	0.0556	0.0461
wR2 [I > 2σ(I)]	0.1451	0.1284
R1 (all data)	0.0728	0.0534
wR2 (all data)	0.1629	0.1376

^a GOF = $[\sum w(F_o - F_c)^2 / (n - p)]^{1/2}$; n = number of reflections, p = number of parameters refined. ^b R1 = $\sum(|F_o| - |F_c|) / \sum |F_o|$; wR2 = $[\sum w(F_o^2 - F_c^2)^2 / \sum w F_o^4]^{1/2}$.

**Figure 5.** UV–visible spectra (in CH₂Cl₂) of **1–3**.

Both transitions have increased molar absorptivity values and also seem to converge. Calculations suggest, however, that the ordering of the transitions are *actually reversed* in **2** and **3** (vide infra). This hypothesis is in fair agreement with time-dependent DFT (TDDFT) calculations, which predict a transition of relatively high oscillator strength ($f = 0.31$) for **3** at 450 nm. The UV–visible spectrum of **6**, by comparison, shows π – π^* and n – π^* transitions at 249, 284, and 364 nm.³⁶

Raman spectra offer support for increased oscillator strengths for the P=P bonds in **2** and **3**. The Raman spectra of **2** and **3** (532 nm excitation, Figure 6) demonstrate that auration additionally shifts the P=P stretching frequency to higher energies relative to **1** (610 cm⁻¹ in KBr disk at 364 nm laser excitation). This shift to higher energy has been previously observed for methylated analogue **6** (638 cm⁻¹ via IR spectroscopy), and in the case of **2**, the measured $\nu_{\text{P=P}}$ agrees well with an observed

**Figure 6.** Raman spectra for **2** (top) and **3** (bottom) at 532 nm laser excitation. Normalized Raman intensity has been plotted as a function of the Raman shift (cm⁻¹). The relative positions of the P=P vibrations have been noted for comparative purposes.

band of moderate intensity in its IR spectrum (648 cm⁻¹). The data thus argue for an increase in the P=P bond strength upon auration. Our computational results, however, did not indicate an increase in phosphorus–phosphorus bonding (vide infra).

The electronic structure of diphosphenes have been investigated theoretically by a number of different groups.^{19,37–39} Calculations at the CCSD(T) level performed on the protonated diphosphene [HP=PH₂]⁺ suggest that the P=P dissociation energy increases by 26% relative to the neutral diphosphene.³⁶ Static and time-resolved DFT calculations were undertaken to probe the fundamental bonding in **1–3**. These calculations were performed on model complexes **1'–3'** where methyl groups replaced the Mes* units on phosphorus. Geometry optimizations proceeded with imposed symmetry: C_s for **2'** and C_{2h} for **3'**. Harmonic frequency calculations confirmed the converged structures to be potential energy minima. Optimized metrics are in fair agreement with experiment. The phosphorus–phosphorus bond lengths are calculated to be 2.047 (**2'**) and 2.044 Å (**3'**), compared to 1.975(5) Å observed experimentally for **2** and 2.003(4) Å for **3**. The phosphorus–phosphorus bond length calculated for free (*E*)–MeP=PMe (**1'**) is 2.056 Å. The calculations thus predict that for each successive gold(I) center that binds, the phosphorus–phosphorus bond contracts. In general agreement with these calculations, Raman spectroscopy suggests that each successive auration strengthens the P=P bond while X-ray crystallography indicates auration shortens the P=P bond, although the effect is not incremental within experimental limits (vide supra).

Figure 7 depicts partial Kohn–Sham orbital energy level diagrams for model complexes **2'** and **3'**. In each, the fragments are held in their local geometries within the optimized complex (i.e., they are not separately optimized), causing slight differences in the fragments' energy levels between **2'** and **3'**. Methylene chloride solvation is treated approximately with the polarized continuum model of Tomasi and co-workers. The highest occupied Kohn–Sham orbital (HOMO) of free **1'** is an n orbital with significant (87%) lone-pair character on phos-

(37) Allen, T. L.; Scheiner, A. C.; Yamaguchi, Y.; Schaefer, H. F., III *J. Am. Chem. Soc.* **1986**, *108*, 7579–7588.

(38) Nagase, S.; Suzuki, S.; Kurakake, T. *J. Chem. Soc. Chem. Commun.* **1990**, 1724–1726.

(39) Sudhakar, P. V.; Lammertsma, K. *J. Am. Chem. Soc.* **1991**, *113*, 1899–1906.

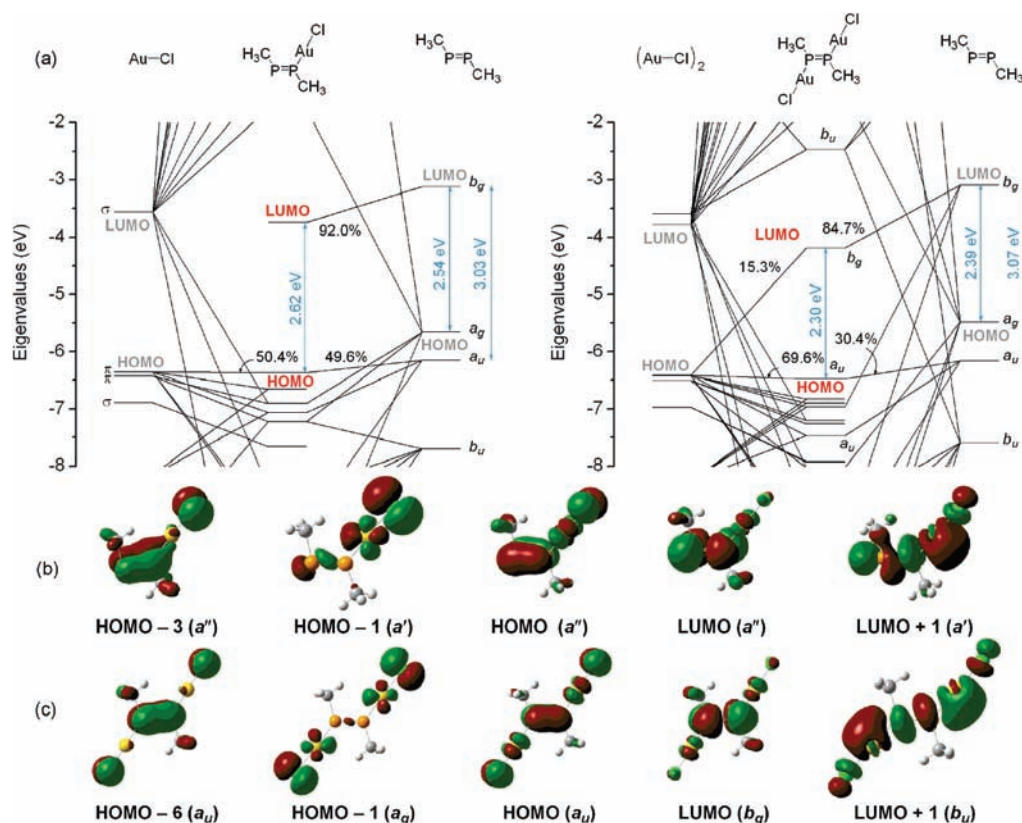


Figure 7. (a) Kohn–Sham orbital correlation diagram of **2'** (left) and **3'**, optimized in C_s and C_{2h} symmetry, respectively. Plots of selected orbitals (0.03 au) of **2'** and **3'** appear below in (b) and (c), respectively.

phorus. This orbital is the in-phase combination of the lone pairs on phosphorus. The antiphase combination is the HOMO -2 ; it is stabilized by overlaps with methyl carbon and hydrogen functions. It lies some 1.9 eV below the HOMO. Upon complexation of one or two gold(I) centers, the diphosphene HOMO drops steeply in energy. The HOMOs of the gold complexes are the phosphorus–phosphorus π -bonding orbitals. The lowest unoccupied Kohn–Sham orbitals (LUMOs) are stabilized upon complexation because of an admixture of chlorogold(I) character. The total HOMO–LUMO gap in either complex is fortuitously similar to that of the free diphosphene ligand, in spite of the orbital changes that occur on complexation.

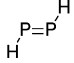
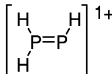
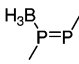
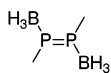
TDDFT calculations on **2'** and **3'** find the lowest-lying singlet–singlet transitions originate from the highest few occupied orbitals to the LUMO. In monogold complex **2'**, the first seven excitations are to the LUMO; in **3'**, the first 10 (Table 2). For both complexes, the highest oscillator strength of any transition calculated past 300 nm occurs for an absorption that is primarily LUMO \leftarrow HOMO in composition. For **2'** this transition, calculated at 398 nm (3.11 eV) carries 59% LUMO \leftarrow HOMO character with a 29% admixture of LUMO \leftarrow HOMO-3 excitation through configuration interaction (the relevant orbitals are plotted in panel b of Figure 7). For digold **3'**, a moderately allowed absorption is calculated at 450 nm (2.75 eV) consisting of LUMO \leftarrow HOMO (71%) and LUMO \leftarrow HOMO -6 (16%) one-electron promotions engaged in configuration interaction. Inspection of Figure 7c shows these orbitals to be analogous to the HOMO-3 and HOMO, respectively, of **2'**. Thus, in both compounds, absorption onset results from a P=P π - π^* transition that also includes π -character from gold and chlorine. The n - π^* absorptions expected for the free

Table 2. TDDFT-Calculated Singlet Excited States, Oscillator Strengths, f , and Compositions in Terms of One-Electron Promotions for Most Significant States^a

Model Compound 2'				
no.	λ (nm)	f	assignment	
1	422.0	0.0001	H-1 \rightarrow L+0 (98%)	
2	398.5	0.1276	H-0 \rightarrow L+0 (59%)	
3	379.3	0.0025	H-2 \rightarrow L+0 (87%)	
4	336.8	0.0066	H-4 \rightarrow L+0 (85%)	
5	312.9	0.0059	H-6 \rightarrow L+0 (94%)	
6	312.5	0.0008	H-5 \rightarrow L+0 (99%)	
7	299.2	0.1121	H-3 \rightarrow L+0 (50%)	
8	263.8	0.0003	H-0 \rightarrow L+1 (67%)	
9	258.6	0.0054	H-7 \rightarrow L+0 (64%)	
Model Compound 3'				
no.	λ (nm)	f	assignment	
1	465.3	0.0000	H-1 \rightarrow L+0 (99%)	
2	453.2	0.0002	H-2 \rightarrow L+0 (99%)	
3	450.5	0.3058	H-0 \rightarrow L+0 (71%)	
4	408.6	0.0000	H-3 \rightarrow L+0 (90%)	
5	402.6	0.0000	H-4 \rightarrow L+0 (98%)	
6	397.0	0.0111	H-5 \rightarrow L+0 (99%)	
7	327.2	0.0057	H-9 \rightarrow L+0 (93%)	
8	326.7	0.0000	H-7 \rightarrow L+0 (99%)	
9	326.6	0.0017	H-8 \rightarrow L+0 (99%)	
10	326.0	0.0000	H-10 \rightarrow L+0 (98%)	
11	314.9	0.0000	H-11 \rightarrow L+0 (90%)	
12	301.1	0.1175	H-6 \rightarrow L+0 (59%)	
13	298.9	0.0000	H-0 \rightarrow L+1 (87%)	
14	275.1	0.1746	H-1 \rightarrow L+1 (92%)	
15	272.6	0.0000	H-2 \rightarrow L+1 (94%)	
16	270.9	0.0046	H-3 \rightarrow L+1 (96%)	
17	266.7	0.0004	H-12 \rightarrow L+0 (95%)	
18	261.9	0.0000	H-0 \rightarrow L+2 (93%)	
19	258.9	0.0000	H-13 \rightarrow L+0 (94%)	
20	251.5	0.1305	H-4 \rightarrow L+1 (92%)	

^a H = HOMO, L = LUMO, L+1 = LUMO+1, etc.

Table 3. Calculated and Experimental P=P Bonding Parameters

Complex	Calculated Bond Length (Å)	Wiberg Bond Order ^b	Forward Donation (e ^b)	Back Donation (e ^b)	P=P, Theoretical (cm ⁻¹) ^c	P=P, Experimental (cm ⁻¹) ^{c,e}
1'	2.056	1.870	NA	NA	576	610(R) for 1' ^f
2'	2.047	1.741	0.506	0.194	601	645(R), 648(IR) for 2' ^g
3'	2.044	1.578	1.094	0.395	619	685(R) for 3
	2.004 ^a (2.055)	-	NA	NA	606 ^a (614) ^d	-
	-	-	-	-	636 ^d	638(IR) for 6 ^h
	2.044	1.783	0.390	0.231	631	-
	2.035	1.625	0.859	0.487	662	-

^a Calculated by two configuration self-consistent field (TCSCF) method. ^b Computed from Dapprich–Frenking charge density analysis. ^c A_g or A₁ mode. ^d At MP2/6-31G(d,p) level of calculation.³⁶ ^e Determined by Raman spectroscopy for **1–3** unless otherwise noted. ^f Literature value. ^g Determined by IR spectroscopy (KBr). ^h Determined by IR spectroscopy (KBr) for compound **6**. R = Raman; IR = infrared.

diphosphene are suppressed because of the stabilizing effect of gold on the phosphorus lone-pair electrons.

A Dapprich–Frenking charge decomposition analysis finds that the gas-phase model diphosphene ligand accepts significant back-donation from the AuCl fragments, although its overall tendency is toward electron donation. For **2'**, a transfer of 0.194 e from AuCl to the diphosphene ligand is calculated; the net charge transfer (which includes σ -donation) of 0.545 e from diphosphene to AuCl. In digold **3'**, (AuCl)₂-to-diphosphene back-donation provides 0.395 e, but net electron transfer is 1.054 e from diphosphene to (AuCl)₂.⁴⁰

Calculation of the Wiberg bond order between phosphorus atoms finds that multiple bond character, however, decreases upon complexation of Lewis acidic fragments. To determine if this effect on P=P bond order requires filled d orbitals, control calculations were performed on hypothetical mono- and diborane adducts (*E*)-Me{BH₃}P=PMe and (*E*)-Me{BH₃}P=P{BH₃}Me. Table 3 reports Wiberg bond orders for mono- and digold(I) chloride complexes of the model phosphene and for the corresponding borane adducts. For comparison, relevant calculated values for *trans*-HP=PH and its monoprotinated analogue are included; the diprotinated dication has not been included, as calculations have indicated this dication is unstable.³⁶ Borane complexation also diminishes the phosphorus–phosphorus bond order but to a lesser degree than gold(I) bonding. Table 3 also collects forward and back electron donations as calculated from Dapprich–Frenking charge decomposition analyses. Significant electron transfer occurs in each direction, between phosphene and Lewis acidic (AuCl or BH₃) fragments. Forward donation from phosphorus to gold exceeds that to boron, whether one or two Lewis acid fragments are bound. Back electron transfer from

boron to phosphorus exceeds that from gold. These calculations concur with elementary ideas about electronegativity. The Pauling electronegativity of boron is 2.0; that of gold is 2.4. The more electronegative atom is more accepting of σ -electron density from phosphorus. This transfer of electron density diminishes σ -bonding between phosphorus atoms and lessens their calculated bond orders. This is corroborated by both theoretically and experimentally determined P=P stretching frequencies for the sets of diphosphenes **2'–3'** and **2–3**, respectively.

While it is commonly assumed that increased force constants and shorter bond lengths reflect increased bond strengths, there have been apparent exceptions noted.^{41–45} For example, protonation of imines can lead to stronger, but longer, CN bonds.⁴⁶ In general, the protonation of AB molecules where B is an atom bearing lone pair(s) has been determined by theory to yield stronger AB bonds.⁴⁷ In addition, the more electronegative the element B (and greater the difference in electronegativity between A and B), the greater the change in bond strength. The apparent contradiction between the computed shorter bond lengths and smaller bond orders suggests that the borane and gold adducts of diphosphene may also represent exceptions to the general wisdom that shorter bonds are stronger bonds.

Pestana and Power have reported interesting compounds displaying unusually shortened PP *single* bond lengths.⁴⁸ Diboryl-substituted diphosphanes, in particular, were shown to have PP bond lengths of about 2.11 Å, below that expected for

(40) The net charge transfers here differ from the forward and back donations appearing in Table 2. The quantities denoted forward donation and back donation include both charge transfer and polarization contributions. Because of these polarization interactions, the net charge transfer between fragments does not equal the difference between forward and back electron donation.

(41) Olah, J.; Blockhuys, F.; Veszpremi, T.; Van Alsenoy, C. *Eur. J. Inorg. Chem.* **2006**, 69–77.

(42) Kaupp, M.; Riedel, S. *Inorg. Chim. Acta* **2004**, 357, 1865–1872.

(43) Kaupp, M.; Metz, B.; Stoll, H. *Angew. Chem., Int. Ed.* **2000**, 39, 4607–4609.

(44) Ernst, R. D.; Freeman, J. W.; Stahl, L.; Wilson, D. R.; Arif, A. M.; Nuber, B.; Ziegler, M. L. *J. Am. Chem. Soc.* **1995**, 117, 5075–81.

(45) Christen, D.; Gupta, O. D.; Kadel, J.; Kirchmeier, R. L.; Mack, H. G.; Oberhammer, H.; Shreeve, J. M. *J. Am. Chem. Soc.* **1991**, 113, 9131–5.

(46) Bond, D. *J. Am. Chem. Soc.* **1991**, 113, 385–7.

(47) Boyd, R. J.; Glover, J. N. M.; Pincock, J. A. *J. Am. Chem. Soc.* **1989**, 111, 5152–5.

standard PP single bonds (ca. 2.22 Å). In these compounds, however, there is notable planarization of the phosphorus atoms compared to conventional diphosphanes, indicative of substantial π -bonding between the B and P atoms. The bond length reduction was ascribed to the rehybridization of the phosphorus σ -bonding orbitals, with possible contributions from increased p–p π -bonding. A reduction in interelectronic interactions between phosphorus atom lone pairs (due to their engagement with the vacant p orbitals on boron) was not considered a primary factor for explaining the PP bond length contraction. For compounds **2** and **3**, the PPC bond angles and CPPC torsional angles are largely unchanged from that of **1** (Figure 3), and thus, rehybridization arguments are harder to justify for these particular compounds. This reasoning leaves open the possibility that gold binding of the phosphorus lone pairs might relieve some interelectronic repulsions involving the now bonded lone pairs.

The above calculations, however, are all self-consistent in that the lone pairs of electrons on phosphorus have been bonded to gold and that the energetics of MOs involved have been significantly lowered. The fact that neither **2** or **3** display appreciable fluorescence cannot be reasonably attributed to fluorescence quenching by the lone pairs. The lack of fluorescence emission and rapid nonradiative decay from **2** and **3** might be associated with changes in the excited state geometries of these molecules. Photophysical studies of **1** has shown that it can undergo both *E*–*Z* isomerization and CH bond insertion of vicinal methyl groups, the ratio of which can be influenced by both temperature and wavelength of exciting light.^{49,50} A

preliminary experiment revealed that a solution of digold diphosphene **3** in CDCl₃ exposed to sunlight for 30 min generates a mixture of **3** and new material having a very broad ³¹P resonance at 272 ppm. The ¹H NMR spectrum shows the new material to be present in nearly equal quantity relative to **3**, and a single set of Mes* resonances (δ 1.24 (s, 9H), 1.48 (br, 18H), 7.21 (t, 2H, *J* = 2 Hz)). This shift is consistent with isomerization to *Z*-**3** that also has some sort of restricted bond rotations occurring on the NMR time scale. Continued exposure of this mixture to sunlight led to other unidentified signals. Further studies are necessary to make conclusive statements.

Conclusions

Facile synthetic protocols for the syntheses of monoaurated and diaurated adducts of the hindered diphosphene **1** have been developed. NMR spectroscopic data are consistent with previous investigations, and X-ray crystallography has unequivocally confirmed the identity of these products, including an unprecedented diaurated adduct **3**. Crystallography and vibrational spectroscopy indicate that auration shortens and strengthens the P=P bonds, respectively. These data were supplemented by DFT calculations on model complexes **1'**–**3'**, which provided a concise corroboration of the spectroscopic and crystallographic data accrued for **1**–**3**, with the exception that smaller bond orders are predicted.

Acknowledgment. We thank NSF for support (CHE-0202040 and CHE-0748982 to J.D.P., and CHE-0749086 to T.G.G.) and for funds to purchase the single crystal X-ray diffractometer used in this study (CHE 0541766), and for Dr. M. C. Simpson (University of Auckland, NZ) for helpful comments.

Supporting Information Available: Crystallographic data for **2** and **3** in CIF format; complete ref 28. This material is available free of charge via the Internet at <http://pubs.acs.org>.

JA900813V

- (48) (a) Pestana, D. C.; Power, P. P. *J. Am. Chem. Soc.* **1989**, *111*, 6887–6888. (b) Pestana, D. C.; Power, P. P. *Inorg. Chem.* **1991**, *30*, 528–535.
- (49) Caminade, A. M.; Verrier, M.; Ades, C.; Paillous, N.; Koenig, M. *J. Chem. Soc., Chem. Commun.* **1984**, 875–877.
- (50) Yoshifuji, M.; Sato, T.; Inamoto, N. *Chem. Lett.* **1988**, 1735–1738.